Supporting Information

Short-process regeneration and utilization of transition metal elements from spent ternary cathode materials after lithium extraction

Table S1. Composition of the solution after acid leaching under optimal conditions.

elements	Ni	Co	Mn	Cu	Al	Fe	Zn	Cr
concentration ($mg\ L^{-1}$)	12038.8	9392.31	5734.46	942.09	1093.64	210	4.44	28.18

Table S2. Leaching kinetics parameters of fitted lines of $1-2/3x-(1-x)^{2/3}$ vs.t.

Temperature(℃)	Ni		Co		Mn	
	k (min^{-1})	R^2	k (min^{-1})	R^2	k (min^{-1})	R^2
25	0.00119	0.99497	0.00193	0.99514	0.00132	0.99307
40	0.00156	0.99773	0.00256	0.99655	0.00194	0.99622
55	0.00202	0.99566	0.00346	0.99714	0.00319	0.99311
70	0.00351	0.99702	0.00418	0.999	0.00409	0.99605
90	0.00537	0.99224	0.00549	0.9933	0.00573	0.99464

Table S3. Leaching kinetics parameters of fitted lines of $1-(1-x)^{1/3}$ vs.t.

Temperature(℃)	Ni		Co		Mn	
	k (min^{-1})	R^2	k (min^{-1})	R^2	k (min^{-1})	R^2
25	0.00548	0.96385	0.00736	0.96071	0.00413	0.97709
40	0.00543	0.98366	0.00781	0.9909	0.00542	0.98433
55	0.00795	0.9908	0.00869	0.99542	0.00729	0.97734
70	0.00993	0.99407	0.00947	0.99905	0.00871	0.99364
90	0.01007	0.99064	0.0876	0.98526	0.00974	0.99125

Table S4. Leaching kinetics parameters of fitted lines of x vs.t.

Temperature(℃)	Ni		Co		Mn	
	k (min^{-1})	R^2	k (min^{-1})	R^2	k (min^{-1})	R^2
25	0.011	0.92498	0.01214	0.90224	0.009	0.95931
40	0.00935	0.93839	0.01148	0.94179	0.00935	0.9533
55	0.01117	0.94672	0.01042	0.93957	0.00939	0.90494
70	0.01043	0.91761	0.00932	0.93819	0.00806	0.92557
90	0.00848	0.89296	0.00577	0.87998	0.00738	0.88289

Table S5. Composition of the solution after impurity removal under optimal conditions.

elements	Ni	Co	Mn	Cu	Al	Fe	Zn	Cr
concentration ($mg\ L^{-1}$)	11217.4	8910.42	5363.17	3.88	3.88	0.92	4.12	3.28

Table S6. The specific parameters of the Rietveld refinement results.

Samples	a	c	c/a	$I_{(003)}/I_{(104)}$	Ni in Li Site
R-NCM@880℃	2.8620	14.2076	4.9642	1.351	3.2%
NCM@880℃	2.8579	14.1951	4.9670	1.405	2.2%

Table S7. The Impedance data of R-NCM@880℃ andNCM@880℃ Samples.

Samples	**Rs(Ω)**	**Rst(Ω)**	**Rct(Ω)**
R-NCM@880℃	2.08	20.6	42.02
NCM@880℃	1.60	33.33	65.65

Table S8. Composition of raw materials

elements	Ni	Co	Mn	Cu	Al	Fe
concentration (%)	18.06	14.09	8.60	1.04	0.98	0.34

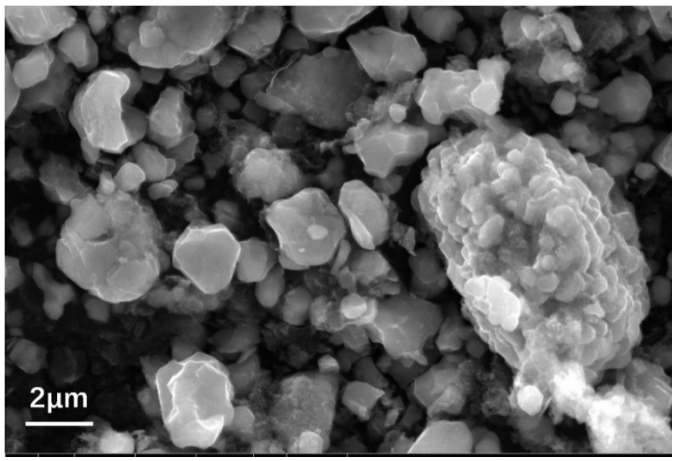

Figure S1. SEM image of cathode materials from spent lithium-ion batteries.

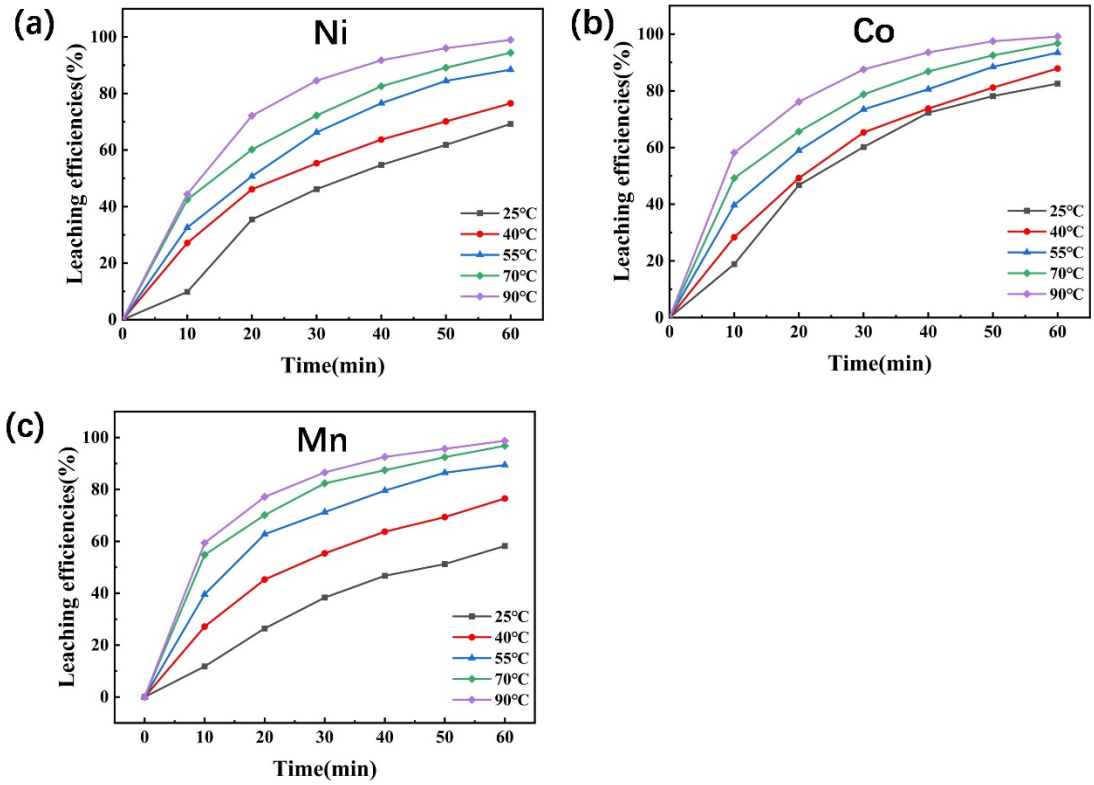

Figure S2. Effects of temperature and time on the leaching efficiency of different valuable metals (a) Ni, (b) Co, (c) Mn

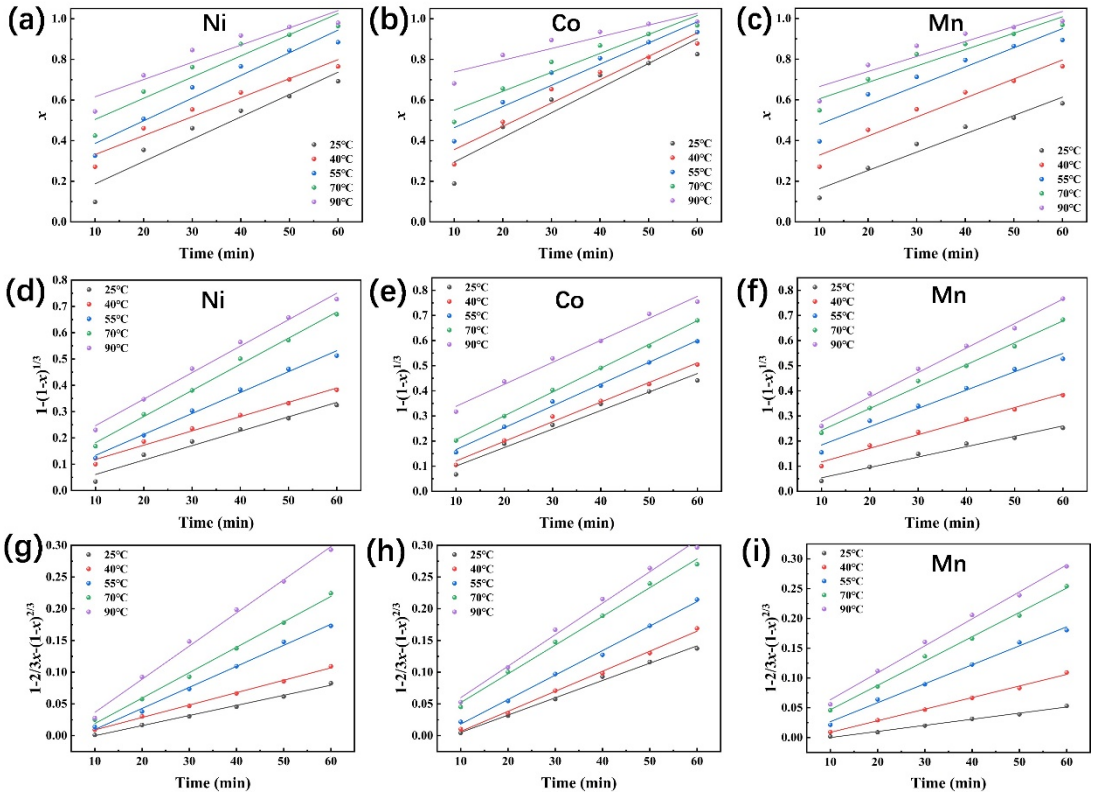

Figure S3. Fitting results of x and t at different temperature (a)Ni, (b)Co, and (c)Mn; Fitting results of $1-(1-x)^{1/3}$ and t at different temperature (d)Ni, (e)Co, (f)Mn; Fitting result of $1-2/3x-(1-x)^{2/3}$ and t at different temperature (g)Ni, (h)Co, (i)Mn.

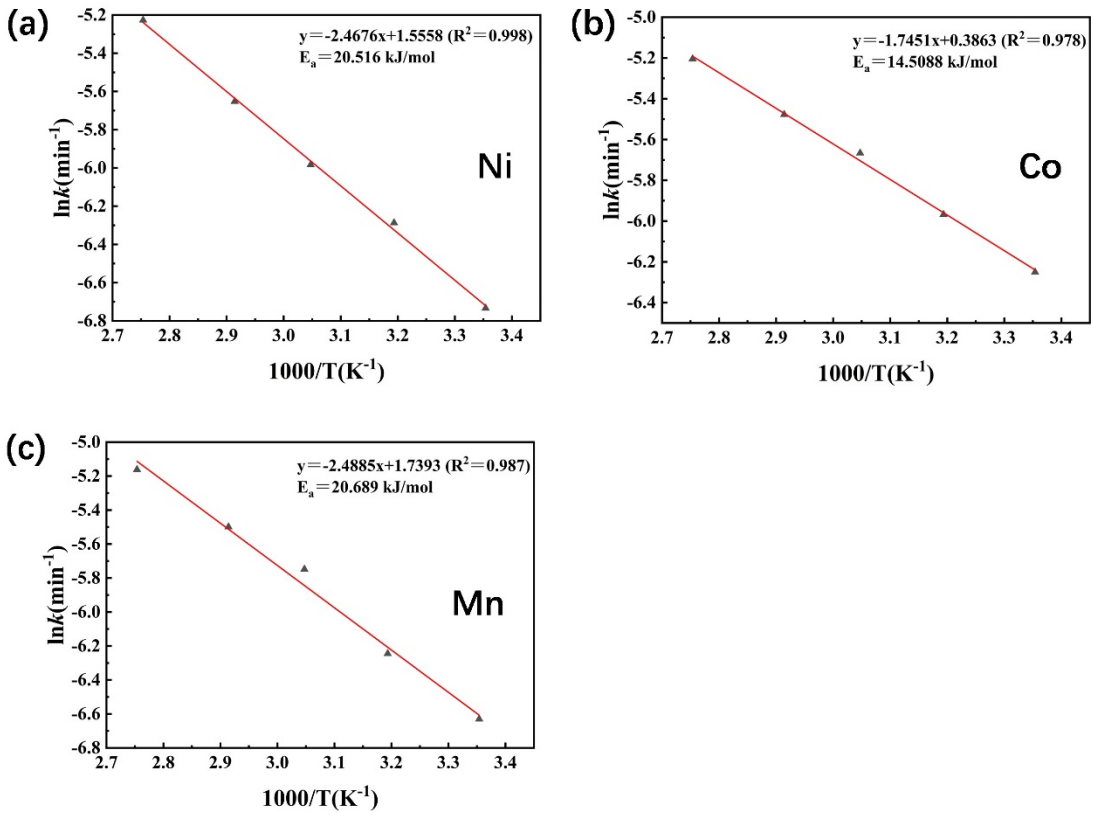

Figure S4. Arrhenius plots for the leaching of valuable metals (a)Ni, (b)Co, (c)Mn.

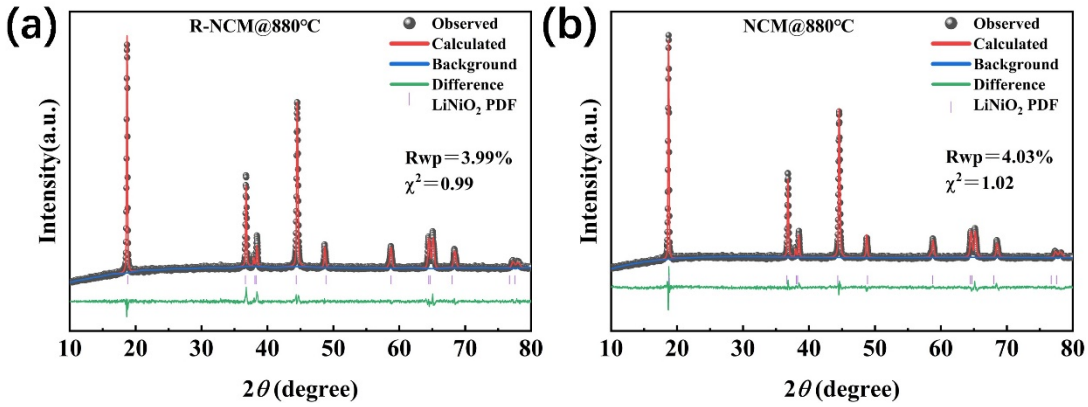

Figure S5. Rietveld refinements of R-NCM@880 (a) and NCM@880℃ (b).

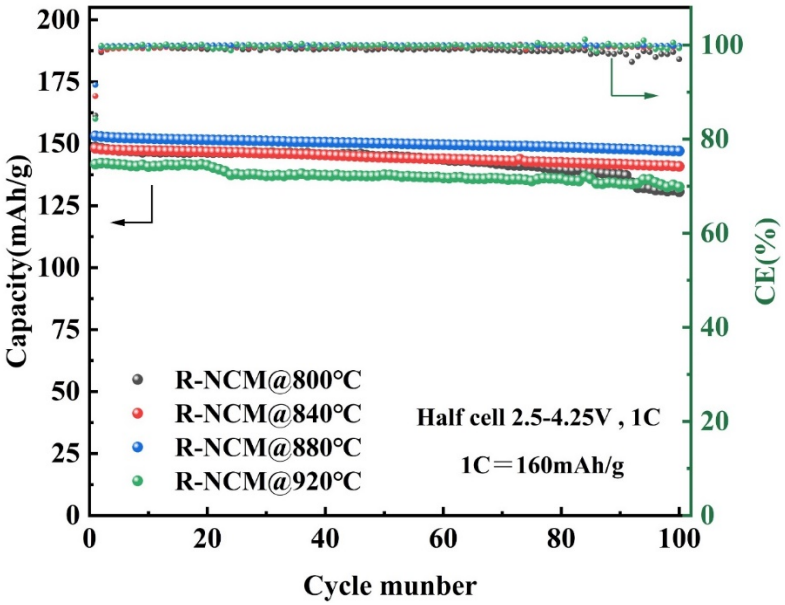

Figure S6. Cycle curves of regenerated cathode materials synthesized at different temperatures.

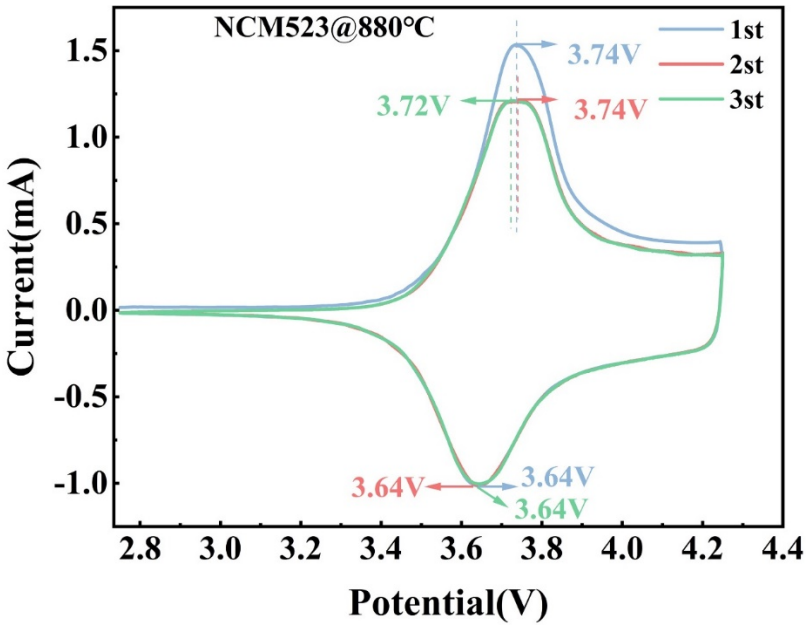

Figure S7. CV curve of commercial cathode material NCM@880°C.

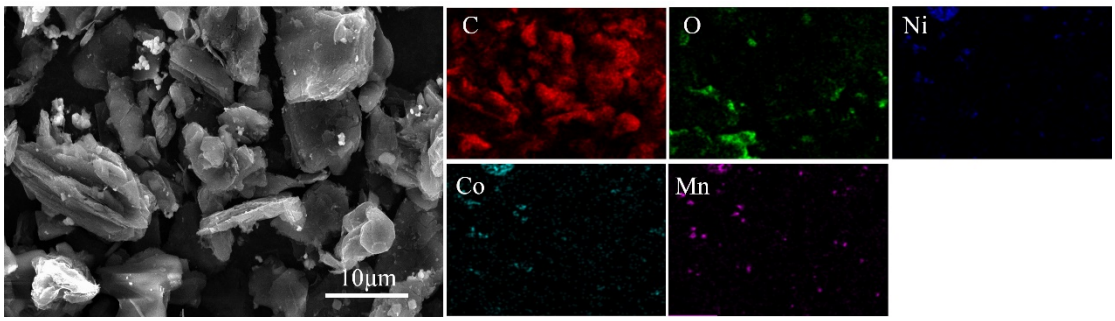

Figure S8. SEM-EDS images of raw materials.

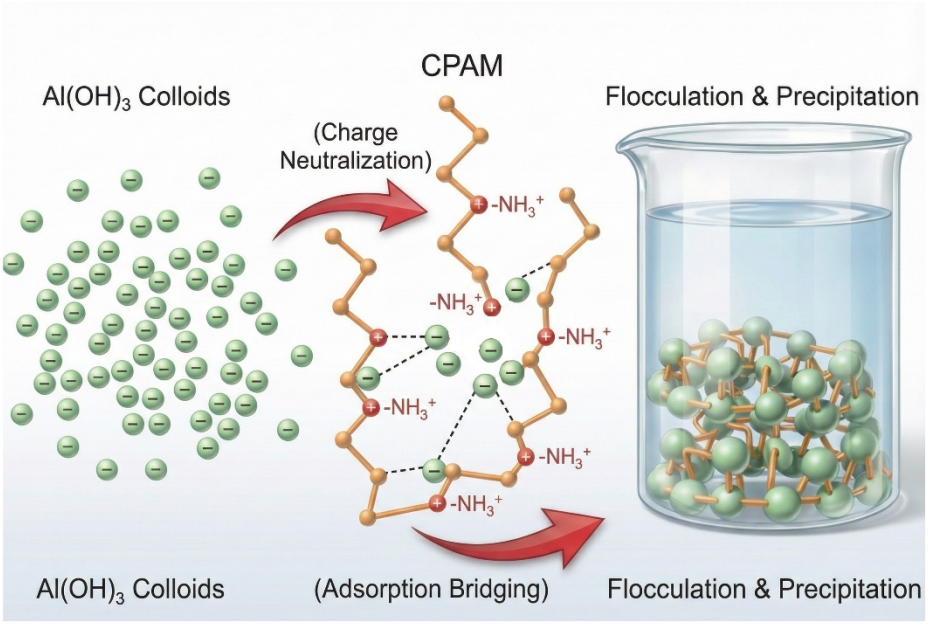

Figure S9. Mechanism Illustration of CPAM-Mediated Flocculation of Aluminum Hydroxide.

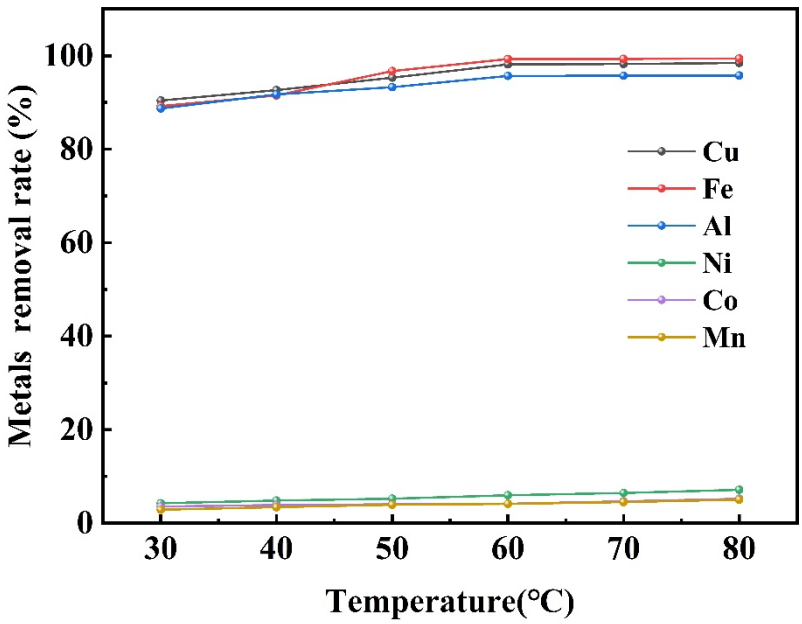

Figure S10. Relationship Between Removal Rate of Metal Precipitates ($M(OH)_n$) and Temperature.

Kinetic studies:

To investigate the leaching kinetics of Ni, Co, and Mn during acid leaching, experiments were conducted at fixed conditions for each variable (sulfuric acid concentration, leaching time, liquid-to-solid ratio, oxidant dosage) under different temperatures (25°C, 40°C, 55°C , 70°C, 90°C) while keeping other variables constant. Samples were collected every 10 minutes over a 60-minute period for ICP analysis of Ni, Co, and Mn. Leaching rates were calculated and plotted as shown in Figure S2. Based on the shrinking nucleus model, the leaching data were fitted using outward diffusion control (Equation 1), a chemical reaction control model (Equation 2), and an inward diffusion model (Equation 3).

$$x = k_1 t \tag{1}$$

$$1 - (1 - x)^{1/3} = k_2 t \tag{2}$$

$$1 - \frac{2}{3}x - (1 - x)^{2/3} = k_3 t \tag{3}$$

x is the leaching rate (%) of different valuable metals; k_1, k_2, and k_3 are the apparent rate constants (min^{-1}); t is the leaching time (min). Typically, the apparent rate of a leaching reaction primarily depends on the slowest step, referred to as the rate-limiting step of the leaching reaction. The leaching data for Ni, Co, and Mn were fitted using the three different kinetic models described above. Figure S3(a–c) shows the fitting results for x versus t at different temperatures; Figure S3(d–f) shows the fitting results for $1-(1-x)^{1/3}$ versus t at different temperatures; Figure S3(g–i) shows the fitting results of $1–2/3x–(1–x)^{2/3}$ versus t at different temperatures. As seen in Figure S3, the linear fitting results for the diffusion-controlled equation are relatively good. The kinetic parameters fitted by the three control models in Tables S2, S3, and S4 indicate that the coefficient of determination R^2 for Ni, Co, and Mn in the internal diffusion-controlled model exceeds 0.99 at every leaching temperature. This demonstrates that the internal diffusion-controlled model exhibits superior fitting correlation compared to the other two models. The apparent activation energy (E_a) for the leaching reaction was calculated using the Arrhenius equation (4):

$$k = A \exp(- E_a/RT) \quad (4)$$

In the equation, A represents the frequency factor, K denotes the reaction rate constant (min^{-1}), E_a signifies the apparent activation energy of the reaction (kJ mol^{-1}), T is the thermodynamic temperature (K), and R is the molar gas constant (8.314 kJ mol^{-1}). Based on the kinetic parameters in Table S2, linear fitting was performed to calculate the apparent activation energies (E_a) for Ni, Co, and Mn, with results shown in Figure S4. Following the Arrhenius equation, plots of the logarithm of the chemical reaction rate constant k for Ni, Co, and Mn at different temperatures versus 1000/T were generated using data from Table 2, as depicted in Figure S4. The determination coefficients R^2 for the fitting results of Ni, Co, and Mn were 0.998, 0.978, and 0.987, respectively. Based on the slopes of the linear equations, the activation energies for the leaching reactions of Ni, Co, and Mn were calculated to be 20.516 kJ mol^{-1} (Ni), 14.509 kJ mol^{-1} (Co), and 20.689 kJ mol^{-1} (Mn).